Parametric generation of energetic short mid-infrared pulses for dielectric laser acceleration

2014 J. Phys. B: At. Mol. Opt. Phys. 47 234016

(http://iopscience.iop.org/0953-4075/47/23/234016)

IOP Publishing Journal of Physics B: Atomic, Molecular and Optical Physics
J. Phys. B: At. Mol. Opt. Phys. **47** (2014) 234016 (10pp) doi:10.1088/0953-4075/47/23/234016

Parametric generation of energetic short mid-infrared pulses for dielectric laser acceleration

S Wandel, G Xu, Y Yin and I Jovanovic

Department of Mechanical and Nuclear Engineering, The Pennsylvania State University, University Park, PA 16802, USA

E-mail: sfw5031@psu.edu

Received 29 May 2014, revised 27 July 2014
Accepted for publication 6 August 2014
Published 24 November 2014

Abstract

Laser-driven high-gradient electron acceleration in dielectric photonic structures is an enabling technology for compact and robust sources of tunable monochromatic x-rays. Such advanced x-ray sources are sought in medical imaging, security, industrial, and scientific applications. The use of long-wavelength pulses can mitigate the problem of laser-induced breakdown in dielectric structures at high optical intensities, relax the structure fabrication requirements, and allow greater pulse energy to be injected into the structure. We report on the design and construction of a simple and robust, short-pulse parametric source operating at a center wavelength 5 μm, to be used as a pump for a dielectric photonic structure for laser-driven acceleration. The source is based on a two-stage parametric downconversion design, consisting of a β-BaB_2O_4-based 2.05 μm optical parametric amplifier (OPA) and a $ZnGeP_2$-based 5 μm OPA. The 2.05 μm OPA is presently pumped by a standard Ti:sapphire chirped-pulse amplified laser, which will be replaced with direct laser pumping at wavelengths >2 μm in the future. The design and performance of the constructed short-pulse mid-infrared source are described. The demonstrated architecture is also of interest for use in other applications, such as high harmonic generation and attosecond pulse production.

Keywords: mid-infrared, $ZnGeP_2$, optical parametric amplifier

(Some figures may appear in colour only in the online journal)

1. Introduction

The current electron accelerator technologies exhibit several important limitations, many of which can be attributed to the relatively low acceleration gradients achievable in conventional radiofrequency (rf)-driven structures. It has been proposed that significantly higher gradients could be achieved by use of optical instead of rf driving fields. In particular, focused pulses produced by short-pulse lasers exhibit a high electric field which could be used to accelerate electrons either directly [1] or by use of intervening plasma perturbations, such as in laser wakefield acceleration (LWFA) [2]. In direct acceleration techniques, either solid-state [3] or transient plasma structures [4, 5] have been considered. One attraction of the direct acceleration techniques in comparison to LWFA is the relatively low required laser peak power, which is compatible with the available and emerging high-repetition-rate, high-average-power laser technology, such as short-pulse fiber lasers [6].

Solid-state-based direct acceleration schemes have received significant attention recently. Designs and simulations of novel optimized photonic bandgap structures have been discussed [7], and proof-of-principle experimental demonstrations of acceleration have been conducted [1, 8]. The photonic bandgap structures that have been proposed and theoretically studied provide the necessary conditions to produce a traveling-wave acceleration field that is phase matched to the injected electrons over an extended distance, while also attempting to maintain favorable transverse beam properties. The desired characteristics of an optically driven

accelerator structure include high damage threshold, high energy loading capability into the fundamental optical mode, and ease of fabrication. The structure performance could be significantly improved and its fabrication challenges could be relaxed by use of longer wavelength laser pulses compared to those produced by traditional near-infrared (IR) short-pulse lasers. By using a mid-IR laser source, multiphoton ionization leading to dielectric structure breakdown can be mitigated. Furthermore, a long driving laser wavelength increases the structure dimensions, thereby permitting larger structure apertures and greater laser pulse energies. Similarly, electron bunches with higher charge can be transmitted through the larger apertures. Novel dielectric laser acceleration (DLA) schemes present a set of other requirements, both on the driving laser pulse and on the structure. The drive laser pulses must efficiently couple to the structure, and a proper phase relationship between the laser and electrons must be maintained along the acceleration length. This can be difficult to achieve, considering the mismatch in both polarization and group velocity of the laser light and the accelerator mode. Additionally, the field strength must be minimized in the coupling region to reduce the probability of material breakdown.

These considerations motivate the development of appropriate mid-IR laser pump sources for DLA. Two main approaches for production of high-energy ultrashort mid-IR laser pulses have been explored to date—the direct production from materials that lase in the mid-IR region and the parametric downconversion/upconversion from a variety of near-IR and visible laser sources or CO_2 lasers. Both approaches are technically challenging for several reasons. The preferred method is the direct mid-IR production from solid-state lasers, including chirped-pulse amplification systems. Promising candidate technologies include mode-locked crystalline solid-state lasers and fiber oscillators based on Cr^{2+}-doped chalcogenides, such as Cr:ZnSe [9] and Cr:ZnS [10], and Tm^{3+}-doped fiber laser [11], respectively. While the direct mid-IR laser pumping of parametric amplifiers is desirable to reduce the system complexity and increase efficiency, the available and proposed high-energy solid-state laser materials exhibit a modest level of maturity at the present time, or do not produce sufficiently long wavelengths or short pulse durations required by applications. For example, a previously developed chirped-pulse regenerative-amplifier system based on Cr:ZnSe has demonstrated production of mid-IR laser pulses centered at 2475 nm with a pulse energy of 0.3 mJ [9]. For certain applications requiring few-cycle mid-IR pulses, the pulse duration from this source may be too long (346 fs). The parametric sources are significantly more versatile, but suffer from lower efficiency, higher complexity, and difficulty in scaling to higher energies (particularly in the case of parametric downconversion). Efficient generation of mid-IR pulses tunable between 1 and 5 μm from 100 kHz-class femtosecond systems has been demonstrated [12]. Pulses with Fourier limits of 50 fs have been produced in the parametric amplification system based on $LiNbO_3$, but the maximum pulse energy achieved within the tunable range has been only 8 μJ at 3.4 μm. Commercial products such as Topas (Light Conversion) offer high-energy variants scalable to up to 50 μJ (signal+idler) in the range of 4–20 μm when pumped by >10 mJ, 100 fs pulses at 800 nm. While the frequency doubling of a CO_2 laser can be used to readily produce 5 μm pulses, the bandwidth limitations of the CO_2 medium limit the pulse durations to few ps. Also, most current applications have preference for solid-state laser media. Common to allapproaches, the atmospheric propagation and the lack and high cost of mid-IR beam and pulse diagnostics instrumentation severely limit the capabilities for production of well-characterized ultrashort mid-IR laser pulses.

Despite the present limitations of sources based on parametric downconversion, they represent both the most viable path for near-term advancement of mid-IR laser-driven accelerators based on dielectric structures and a necessary component of future drive lasers. Even in those drive laser systems that will incorporate mid-IR laser pumps, parametric conversion will remain necessary for extending the operation to longer wavelengths. Operation in the mid-IR (5 μm) range with short pulses (<1 ps full-width-at-half-maximum (FWHM)), high pulse energy (<500 μJ) and good beam quality is required for this specific implementation of DLA. To address this need, we present an approach for production of high-energy ultrashort mid-IR laser pulses at a center wavelength of 5 μm designed to take advantage of mid-IR pumping by 2–2.5 μm pump lasers, such as the Cr:ZnSe laser. Our demonstration utilizes the present mature Ti:sapphire laser pump technology to develop a surrogate 2 μm pump and demonstrate 5 μm mid-IR pulses compatible with one of the recently proposed acceleration approaches [7].

An intermediate achievement with related architecture is also described, which allows the generation of stable 2 μm pump pulses in β-BaB_2O_4 (BBO) that enable the use of high-performance nonlinear crystals transparent only at longer wavelengths, followed by the description of the progress on the design, construction, and operation of a 5 μm parametric source based on $ZnGeP_2$ (ZGP), capable of generating pulses in the range of a few hundred μJ for direct laser acceleration. In addition to DLA applications, we note that the demonstrated mid-IR architecture holds a significant promise for use in high harmonic generation and attosecond pulse production.

2. Mid-IR short pulse generation by optical parametric amplification (OPA)

The most critical considerations in the design and operation of parametric systems include the availability and performance of the pump laser and of the nonlinear conversion materials. Short-pulse OPA offers a flexible approach to access the mid-IR spectral region in a relatively simple design, with the ability to use a single commercially available mature short-pulse pump laser, such as Ti:sapphire or Yb:glass. Unfortunately, the effective OPA crystal dimensions are restricted because the temporal and spatial walk-off of the multiple ultrashort pulses in the three-wave mixing process significantly limits the effective interaction length. Noncollinear operation can be employed to allow the simultaneous group

velocity and phase velocity matching [13]. Although this approach introduces an additional degree of freedom not afforded by a collinear configuration, it causes a spatio-temporal mismatch among the pulse fronts of the three interacting pulses. Additional pulse front tilt compensation can be used to overcome this problem [14]. The pulse duration in short-pulse OPA is primarily governed by the pump pulse length, with some broadening possible due to group velocity mismatch (GVM) among the interacting pulses. Thus the use of a short pump pulse usually results in a short signal pulse, even without extensive dispersion management.

The spatiotemporal distortions present in short-pulse OPAs are greatly reduced and usually insignificant when the technique of optical parametric chirped-pulse amplification (OPCPA) [15] is used. In OPCPA, stretching of the signal to much longer (ps–ns) pulse durations enables the scaling of short pulses to high energies by use of a longer-pulse, high-energy pump. Since the pulses interacting in the OPA crystal are relatively long, the sensitivity of the OPA to inter-pulse delay is reduced. The use of OPCPA in a noncollinear configuration is also relatively straightforward because of the greatly reduced relative spatio-temporal walk-off. However, OPCPA systems usually employ multiple lasers to produce a short seed pulse and a long pump pulse [16]. Electronic synchronization of two laser systems can be challenging; one solution that has been developed is the use of a fraction of the signal laser pulse to seed the pump laser [17]. Dispersion management is more complex in OPCPA, as in any chirped-pulse amplification system that employs a significant stretching factor, whereas it may be entirely circumvented in many short-pulse OPA designs. Even though broad gain bandwidth and favorable phase matching in certain nonlinear crystals have been used to realize few-cycle mid-IR laser pulses, many of the proposed and demonstrated schemes to date rely on complex pump lasers and system designs that incorporate multiple lasers for OPCPA [18, 19].

Multiple stages of OPA are usually needed to produce high gain. This is a consequence of the effective interaction length limited by GVM, limitation on the pump intensity due to crystal damage and high-order nonlinear effects, and parasitic optical parametric generation (OPG). The parametric gain, G, of a monochromatic, perfectly phase-matched OPA is

$$G = \frac{1}{4}\exp\left(2\,L_{\mathrm{eff}}\sqrt{\frac{8\pi^2 d_{\mathrm{eff}}^2 I_{\mathrm{p}}}{n_{\mathrm{p}} n_{\mathrm{s}} n_{\mathrm{i}} \lambda_{\mathrm{s}} \lambda_{\mathrm{i}} \epsilon_0 c_0}}\right), \tag{1}$$

where L_{eff} is the effective interaction length, d_{eff} is the effective nonlinearity, I_{p} is the pump intensity, n_{p}, n_{s}, and n_{i} are the refractive indices for the pump, signal, and idler, respectively, λ_{s} and λ_{i} are the signal and idler wavelengths, respectively, ϵ_0 is the vacuum permittivity, and c_0 is the speed of light in vacuum. Let us consider a BBO crystal and the type-I mixing process 400 nm (e) → 800 nm (o) + 800 nm (o). If 50 fs pulses are used, the effective interaction length for this process limited by GVM is ~260 μm. With an effective nonlinearity of 2.00 pm V^{-1} for this process, an intensity of ~2200 GW cm^{-2} would be needed to produce a gain of 10^6, well above the damage threshold of the BBO crystal. It is also well known that employing a single high-gain OPA crystal produces a large parasitic OPG pulse, which competes with the seeded mode for pump energy conversion. OPG can be greatly reduced in a multi-stage design, where the OPA stages are sufficiently separated for the angularly divergent OPG pulse to be poorly coupled between subsequent stages, or a spatial filtering is employed between stages to selectively remove the divergent OPG pulse.

While many of the distinct characteristics of OPA and OPCPA may make one or the other approach suitable for a particular application, we have adopted a short-pulse two-stage down conversion OPA scheme for the development of a 5 μm pump for the DLA. The choice of OPA over OPCPA is based on the ability to meet the requirements for DLA [7] with as simple design as possible. Since a high acceleration gradient can be achieved in the dielectric structure even with sub-mJ short pulses, high energy scalability is not a priority and subsequently this distinct advantage of OPCPA is not of significant benefit in this application. The use of a multi-stage short-pulse OPA design allows the dispersion management to be significantly simplified, since the final pulse duration is governed primarily by the interaction between the short-pulse pump and signal in the last OPA crystal. The short-pulse OPA approach also allows easy spectral tunability by adjusting the delay between the short pump pulse and the stretched seed (signal) pulse. However, the spatiotemporal distortions in the last crystal must be managed, either by use of pulse front tilt or, in our case, a nearly collinear mixing configuration.

3. Mid-IR gain media and dispersion considerations

Production of few-cycle mid-IR laser pulses has been achieved with a variety of nonlinear optical crystals, such as ZGP [20], $AgGaS_2$ (AGS) [21], $KTiOAsO_4$ (KTA) [18], GaAs [22], BiB_3O_6 (BiBO) [23], and BBO [24]. The notable characteristics of selected common high-performance nonlinear crystals in representative nonlinear mixing processes suitable for production of mid-IR pulses are shown in tables 1 and 2, categorized by the capability for near-IR and mid-IR pumping, respectively. The important characteristics include the transparency range, ability to phase match the combination of the signal, pump, and idler wavelengths by crystal birefringence, the effective nonlinearity, damage threshold, and pulse splitting length. The interaction length over which parametric amplification occurs is constrained by the GVM among interacting pulses and is expressed as the pulse splitting length L_{jp}:

$$L_{\mathrm{jp}} = \frac{\tau}{\left|1/v_{\mathrm{gj}} - 1/v_{\mathrm{gp}}\right|}, \quad j = s, i, \tag{2}$$

where τ is the pump pulse duration, while v_{gj} and v_{gp} are the group velocities of the signal/idler and pump. The pulse splitting length usually sets the maximum effective amplification length in short-pulse OPAs. As seen in tables 1 and 2,

Table 1. Optical characteristics of select high-performance nonlinear crystals used as short-pulse OPAs pumped by near-IR laser pulses for several representative mixing processes. Pulse splitting length is calculated for a 60 fs pump pulse duration. Damage thresholds reported are for 10 ns pump pulses at 1064 nm.

Crystal	Transparency range (nm)	λ_p (μm)	λ_s (μm)	d_{eff}	L_{GVM} (mm)	Damage threshold (GW cm^{-2})	Ref.
BBO	300–2500	0.8	2.05	1.94	3.00	5	[25]
		1.0	2.05	1.86	1.12		
BiBO	300–2500	0.8	2.05	2.11	17.99	0.3	[26]
		1.0	2.05	2.05	0.90		
KTA	350–4000	0.8	4.0	−1.94	0.95	1.5	[27]
		1.0	4.0	−1.96	1.28		

Table 2. Optical characteristics of select high-performance nonlinear crystals used as short-pulse OPAs pumped by mid-IR laser pulses for several representative mixing processes. Pulse splitting length is calculated for a 60 fs pump pulse duration. Damage thresholds reported are for 10 ns pump pulses at 10.6 μm.

Crystal	Transparency range (nm)	λ_p (μm)	λ_s (μm)	d_{eff}	L_{GVM} (mm)	Damage threshold (GW cm^{-2})	Ref.
ZGP	2000–10000	2.05	5.0	77.3	0.40	0.3	[28]
		2.5	5.0	81.1	1.06		
AGS	500–11000	2.05	5.0	8.16	4.50	0.2–0.5	[29]
		2.5	5.0	8.13	2.25		
GaAs	1500–16000	2.05	5.0	70	0.17	0.1	[30]
		2.5	5.0	70	0.30		

the pulse splitting lengths for 5 μm pulse production with mid-IR pumped nonlinear OPA crystals are generally shorter than that for pulse production near 2 μm with near-IR pumping. This presents a particular motivation for using multiple amplification stages to distribute the needed high gain across several OPAs, so that only a modest level of gain is necessary and achievable in each stage with intensities far below threshold for significant OPG or crystal damage. In this way, a multi-stage OPA can provide high energy output at 5 μm and longer wavelengths with pump intensities below ~100 GW cm^{-2} for fs pulses.

Direct pumping using a near-IR pump laser to produce mid-IR pulses is possible in some crystals, such as BBO, BiBO, and KTA; however, their transparency range and/or phase matchability is typically limited to shorter wavelengths (table 1). To obtain longer wavelengths (near 5 μm) for accelerator applications, different nonlinear optical materials, such as ZGP, AGS, and GaAs, are needed, which themselves require mid-IR (>2 μm) pumping. Short pump pulses in the range 2–2.5 μm can be produced either directly from a mid-IR laser (with the 2.5 μm Cr:ZnSe laser being one prominent example [9]), or by another parametric source, including those that can be near-IR pumped (table 1).

BBO and BiBO are frequently used for production of mid-IR pulses using near-IR pump lasers. They are limited to wavelengths shorter than 2–2.5 μm due to crystal transparency. BBO is particularly attractive for multiple reasons that extend beyond its favorable optical properties, including mature growth and fabrication techniques, relative cost-effectiveness, and availability of large apertures. BiBO has favorable dispersive properties when pumped by Ti:sapphire lasers at 800 nm because the zero dispersion wavelength (1580 nm) is near the degeneracy point of Ti:sapphire, thereby minimizing GVM between the signal and idler in a type-I mixing configuration. As a result, amplification at 1.6 μm in a collinear geometry is extremely broadband in BiBO. The nonlinear coefficient for BiBO is comparable to BBO when pumped at 800 nm; however, the available crystal apertures for BiBO are currently limited and the material is higher in cost compared to BBO. KTA has been used to produce 8 mJ few-cycle laser pulses centered at 3.9 μm in an OPCPA scheme [18], but is not transparent above ~4 μm.

Operation at longer wavelengths requires the use of different materials with favorable transparency and phase matching characteristics. A comparison of the optical properties of some of the common nonlinear crystals that can be used to produce mid-IR pulses at wavelengths that extend as far as 16 μm is provided in table 2. The high effective nonlinearity and relatively high damage threshold makes ZGP an attractive crystal for mid-IR generation. AGS does not exhibit a nonlinearity as high as ZGP; however, its transparency at shorter wavelengths makes it possible to pump with a greater range of lasers. GaAs is particularly well-suited for the frequency conversion of laser pulses with relatively high average powers, such as those from continuous-wave lasers or diode-pumped solid-state lasers, but the damage threshold is relatively low. Due to the excellent optical characteristics of ZGP for 5 μm pulse production, in addition to the relatively small GVM among the three interacting pulses in ZGP, as seen in figure 1(a), this crystal is an attractive candidate for parametric amplification of mid-IR laser pulses. Using the determined GVM, the pulse splitting length has been calculated for a 2.05 μm pump with a pulse duration of 60 fs and is shown in figure 1(b). The relatively long effective interaction length allows for the reduction of the required pump intensity to achieve high gain in ZGP crystals.

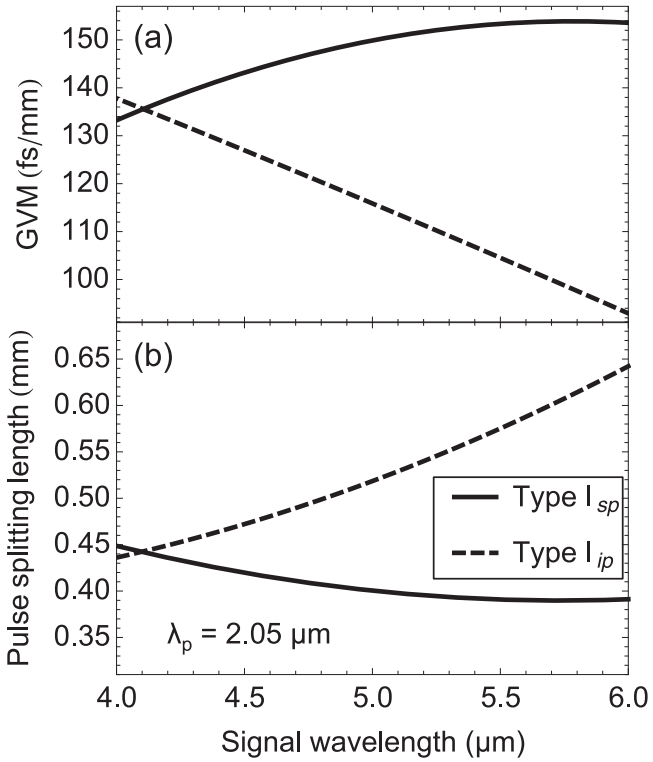

Figure 1. Calculated (a) GVM and (b) pulse splitting lengths for signal-pump and idler-pump as a function of signal wavelength for type-I ZGP OPA pumped by 60 fs, 2.05 μm pulses. Solid line: pump-signal in type-I OPA; dashed line: pump-idler in type-I OPA.

In short-pulse OPAs it is desirable to maintain short pulse durations throughout the system, minimizing the need for additional complex dispersion control. Dispersion and transparency of common optical materials used in the near-IR spectral region can be unfavorable for operation in the mid-IR region. Such materials are needed for the ancillary linear optical system components such as lenses, windows, and beamsplitters. Figure 2 shows the calculated dispersion of common materials used both in the near-IR and the mid-IR spectral region. Whereas SiO_2 and BK7 exhibit a group velocity dispersion (GVD) of 25 and 28 $fs^2\ mm^{-1}$ at 1 μm, respectively, their GVD at 5 μm is significantly greater in magnitude (−7924 and −6685 $fs^2\ mm^{-1}$, respectively). While the GVD of some materials is positive in the near-IR spectral region, it becomes negative in the mid-IR part of the spectrum. For example, the GVD of CaF_2 becomes negative at wavelengths exceeding 1.5 μm. Some optical materials that exhibit relatively low GVD near 5 μm include ZnSe and ZnS (−19 and 54 $fs^2\ mm^{-1}$, respectively). Therefore, careful material selection is needed to simplify and improve the system design and performance.

4. Ultrashort mid-IR source architecture

A 2.05 μm ultrashort pump source to serve as a surrogate for future 2.5 μm Cr:ZnSe pump laser has been developed using the widely available and relatively inexpensive BBO crystals.

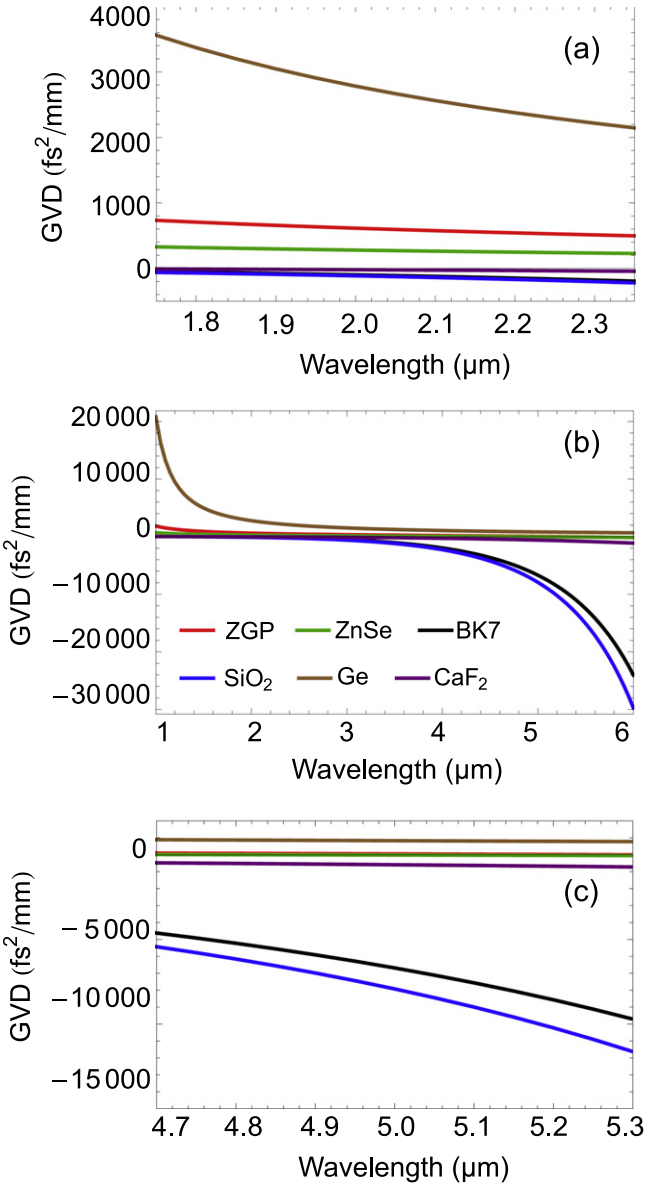

Figure 2. GVD of common materials used in optical elements: (a) near 2.05 μm, (b) within the near-IR and mid-IR spectral range, and (c) near 5 μm. ZGP: red; ZnSe: green; BK7: black; SiO_2: blue; Ge: brown; CaF_2: purple.

The wavelength of the surrogate source is chosen to be within the transparency and phase matching range of both the chosen 5 μm OPA crystals (ZGP) and the BBO. While the surrogate pump source operates at a somewhat shorter wavelength than a Cr:ZnSe laser, it nevertheless allows experimental validation of the performance characteristics of the 5 μm source architecture, and minimal changes to the setup will be required when replacing the surrogate source with a Cr:ZnSe laser in the future. The surrogate pump source is based on a two-stage BBO nondegenerate OPA design with a mixed phase matching scheme [31]. The OPA is pumped by a commercial Ti:sapphire chirped-pulse amplification system (Trident X, Amplitude Technologies), producing 40 fs, up to 14 mJ pulses centered at 800 nm, with a FWHM bandwidth of ~25 nm at a repetition rate of 10 Hz. Two BBO crystals with

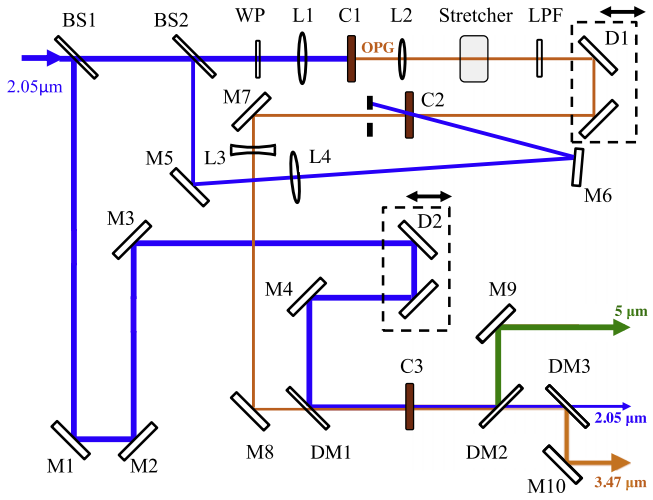

Figure 3. Experimental setup of the two-stage OPG/OPA. Blue: 2.05 μm pump beam; green: 5 μm idler beam; orange: 3.47 μm signal beam. BS—beamsplitter; WP—$\lambda/2$ waveplate; DM—dichroic mirror; LPF—long-pass filter; C—type-I ZGP crystal.

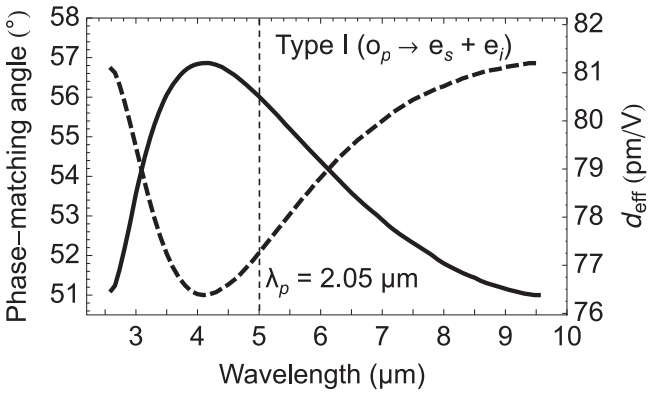

Figure 4. Calculated phase-matching angle (solid) and effective nonlinearity (dashed) for type-I phase-matching in a ZGP crystal to produce 5 μm pulses while being pumped with 2.05 μm laser pulses.

dimensions of 5 × 5 × 2.5 mm^3 and 15 × 15 × 2.0 mm^3 have been used in the first and second stage OPAs, respectively. The crystals were cut at an angle of $\theta = 19.8°$ for type-I ($e_p \rightarrow o_s + o_i$) phase matching and $\theta = 25.9°$ for type-II ($e_p \rightarrow o_s + e_i$) phase matching in the first and second stage OPA, respectively. A portion of the pump beam energy is used to produce a white-light continuum (WLC), from which a fraction of the spectrum can be selected for amplification in consequent OPA stages. Because of the slightly elliptical beam profile of amplified 2.05 μm pulses in a collinear OPA configuration that arises from the tilted pulse front, perhaps due to imperfect WLC production and/or transport, we employ a small (0.4°) tilt between the seed and the pump in both OPA stages to achieve a high conversion efficiency and uniform beam profile. OPAs with noncollinear geometry can achieve broad phase-matching bandwidth at the cost of introducing idler angular dispersion [32]. We therefore chose to seed the OPA using 2.05 μm pulses from WLC, eliminating the need to manipulate the angularly dispersed idler pulse.

The optical design of the 5 μm parametric source is displayed in figure 3. The calculated GVM and pulse splitting lengths in ZGP are shown in figures 1(a) and (b) for type-I phase matching only since type-II phase matching is not possible at 5 μm for a ~2 μm-pumped ZGP. Two ZGP crystals with dimensions of 10 × 10 × 1.0 mm^3 and 10 × 10 × 1.5 mm^3 have been selected for the first and the second stage OPA, respectively. Each crystal is cut at an angle of $\theta = 56.1°$ for type-I ($e_p \rightarrow o_s + o_i$) phase matching with a corresponding effective nonlinearity of 77.3 pm V^{-1}, as shown in figure 4. Both OPA crystals are coated for all three wavelengths present in the OPA process. The beam transport between the surrogate source output and the 5 μm short-pulse OPA system input includes two mirrors, resulting in 93% of the surrogate pump source energy transmitted to the 5 μm OPA. The pump pulse energy is split by two beamsplitters (BS1 and BS2); the pulse transmitted by BS2 is used to produce the OPG that serves as the pump in the first OPA stage. After passing through a half-waveplate to rotate the polarization and an iris diaphragm to block the back reflection from the OPG crystal, the pump pulse with an energy of 25 μJ is focused onto a 1 mm thick ZGP crystal by a lens with a focal length of 100 mm to produce an OPG signal centered at 3.47 μm. We observe a single filament formed within the crystal when the pump pulse energy of 25 μJ is used. At higher incident powers, two or more filaments can be observed. We use an iris size corresponding to the size of a single filament to generate stable white-light seed continuum. We have also considered the use of self-phase modulation in sapphire plate for seed pulse production; however, under identical pumping conditions, OPG produced higher seed pulse energy with better energy stability. The generated seed pulse is collimated with a CaF_2 lens and stretched by use of a 5 mm thick Ge window with dispersion of 1277 fs^2 mm^{-1} at 3.47 μm, enabling selective amplification of different portions of the OPG spectrum in the subsequent OPA by adjusting the seed-pump delay. OPGs exhibit temporal incoherence; however, the coherence is enhanced subsequent to OPG by chirping the OPG pulse and selecting a small temporal/spectral portion of the stretched OPG pulse for frequency mixing in the first OPA. The residual pump beam energy is removed from the OPG signal pulse with a 1 mm thick long-wave-pass filter (LP-3000 nm, Spectrogon). The near-IR absorption of the ZGP crystal is low (~0.04 cm^{-1}) at 2.05 μm [33]. Accordingly, in the single-pass OPG configuration, linear absorption losses for a pump wavelength of 2.05 μm never exceed 1%. The stretched OPG seed pulse with an energy of ~230 nJ is then directed to the first OPA via a delay line. The pump pulse with an energy of 330 μJ reflected by BS2 is focused onto the first OPA crystal by a 500 mm focal length lens. Due to spatial constraints, the smallest noncollinear angle that could be employed in this setup is ~4.6°. The position and angular orientation of the crystal is optimized for maximum conversion efficiency in the first OPA stage, but sufficiently far from the position where significant OPG could be produced. Consequently, the output signal pulse from the first OPA stage at 3.47 μm has an energy of ~23 μJ—of which ~15.7 μJ is transported to seed the second OPA. By

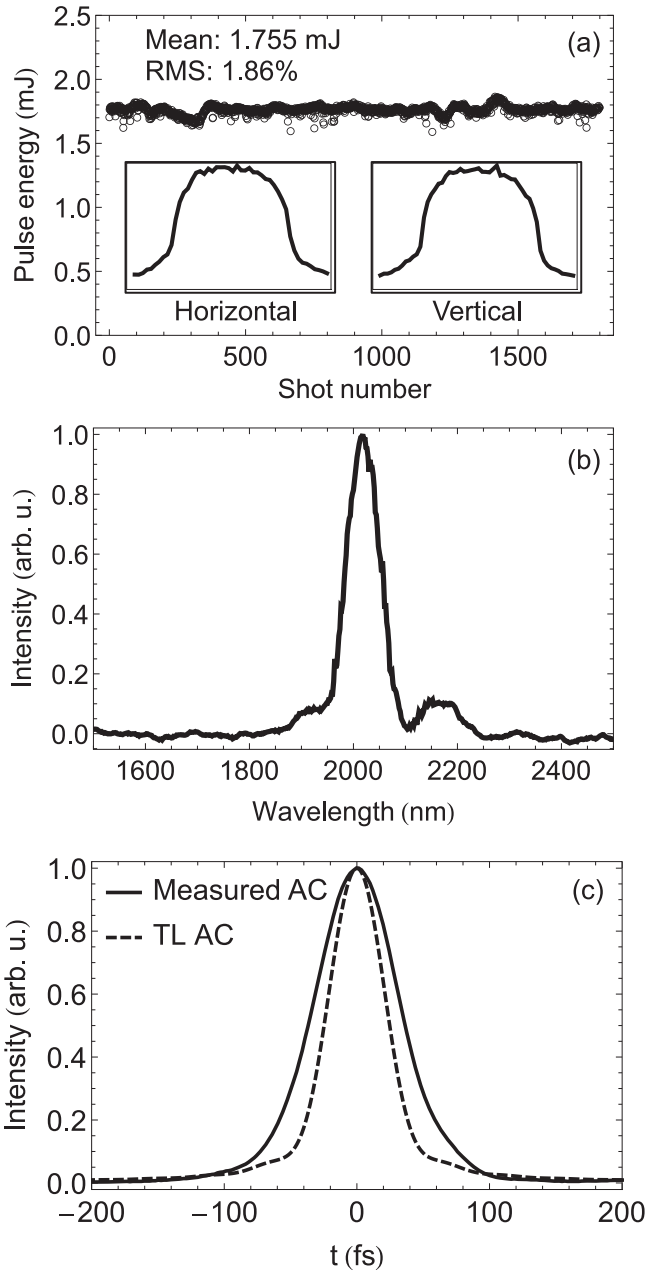

Figure 5. Energy stability of (a) 2.05 μm pump pulses; inset: horizontal and vertical beam profiles, (b) amplified pump pulse spectrum, and (c) autocorrelation of the amplified 2.05 μm pulses. Solid line, experimental measurement; dashed line, transform-limited autocorrelation calculated from the measured spectrum.

using a noncollinear configuration in the first OPA stage, along with an iris diaphragm placed directly behind the first OPA crystal, the residual pump beam is easily removed, while the preamplified signal is directed to the second OPA stage.

The majority of the pump laser pulse energy (~1.3 mJ) is reflected by BS1 and directed to the second OPA stage via another delay line, using a CaF_2 focusing lens with a thickness of 1 mm to resize the beam diameter onto the second OPA. To match the beam diameter of the first OPA stage with that of the high-energy 2.05 μm pump pulse (~7 mm at $1/e^2$) in the second OPA, a beam resizing telescope was used to increase the signal beam size after the first OPA. A dichroic beam combiner is used to overlap the pump beam and the preamplified signal beam in the second OPA crystal. A small noncollinear angle (10 mrad) is employed in the second OPA, which was experimentally determined to maximize the conversion efficiency. We estimate the resulting spatial chirp of order 200 nm across the beam profile of the 5 μm idler, i.e. the shift of center wavelength by 4% of the center wavelength from one edge of the beam to another. The equivalent angular dispersion is 0.17 mrad. We note that a more extensive optimization of the first OPA may allow the complete elimination of spatial chirp in the second stage in the future. Using this source architecture, dispersion management is relatively straightforward and necessary only in the final OPA stage and thereafter. While the OPG process does not preserve the carrier-envelope phase (CEP), a cascaded three-wave mixing scheme employed results in automatic, passive CEP stabilization. Because a CaF_2 focusing lens with a length of 2 mm and a BK7 dichroic beam-combiner with a thickness of 3 mm were used in the preamplified signal pulse beam path, dispersion can not be neglected, and some broadening of the pulse is expected in the second OPA crystal. Finally, the amplified pulses at 5 μm, 3.47 μm, and the residual pump pulse are separated using two dichroic mirrors.

5. Summary of experimental results and outlook

In BBO, type-I phase matching has ~23% higher effective nonlinearity and ~3.5× broader phase matching bandwidth for 2.05 μm pulse production than type-II phase matching when pumped at a wavelength of 800 nm. This is favorable for achieving high parametric gain and shorter pulse durations. The parasitic second-harmonic generation (SHG), however, reduces the output pulse energy and degrades the beam quality. By using a mixed-type two-stage OPA scheme for the surrogate 2 μm pump source, the parasitic SHG is effectively suppressed for both the signal and idler pulses due to the relatively large difference between the phase matching angles of the OPA and the SHG, in addition to the mismatched polarization of the signal pulses for the SHG process. As a result, pulses centered at a wavelength of 2.05 μm with an energy of 2.2 mJ, uniform beam profiles, pulse duration of 43 fs, and rms energy stability of 1.1% have been measured. The 2.05 μm pulses have a FWHM bandwidth of 260 nm, potentially supporting pulses as short as 32 fs, with the corresponding calculated autocorrelation FWHM of ~43 fs.

An available AGS crystal with a thickness of 2 mm and a cut angle of $\theta = 50°$ has also been tested for seed pulse generation via OPG. The AGS crystal is coated with broadband anti-reflective coatings (1.1–2.6 μm and 2.6–11 μm) at the entrance and exit surfaces, respectively, and can also be used in a type-I phase-matching configuration. Energy measurement of both the 2.05 μm pump pulses and the 5 μm signal pulses have been conducted using a pyroelectric detector, providing a sensitivity of ~20 nJ. Spectral properties of the 5 μm idler pulses collected by an uncoated CaF_2 lens

are analyzed using a 0.55 m monochromator with a 300 mm^{-1} grating blazed at 4 μm, in combination with a thermoelectrically cooled InSb photodetector. The output energy of the 5 μm pulse produced by AGS OPG was below the noise level of our pyroelectric detector and could not be directly measured. However, by replacing the AGS with a ZGP crystal in the same setup, the OPG 5 μm pulse energy was well above the noise threshold of the detector. Consequently, the design uses a ZGP crystal with dimensions of $10 \times 10 \times 1.0\ mm^3$ to produce OPG and seed the first OPA.

To realize the most efficient amplification in this two-stage OPA design employing ZGP crystals, the crystal thicknesses at each OPA stage were experimentally varied. We first implemented a design that used a 1.5 mm thick ZGP crystal in the first OPA stage and a 1.0 mm thick ZGP crystal in the second OPA stage. The effective interaction length is limited by the GVM among the three interacting pulses. Even though the preamplified signal from the first OPA resulted in a pulse energy ~5 μJ higher for the scheme utilizing a 1.5 mm thick ZGP crystal than that which uses a 1.0 mm thick ZGP crystal in the first OPA, the final amplified pulse energy for the combined signal and idler pulses was ~40 μJ higher for the scheme utilizing a 1.0 mm thick ZGP crystal in the first OPA stage and a 1.5 mm thick ZGP crystal in the second OPA stage. The latter configuration was subsequently chosen for the 5 μm OPA design.

The 2.05 μm pump pulses and crystal angle orientations have been varied to investigate the effect on production of 5 μm pulses. The 2.05 μm surrogate source produces the maximum energy by using the shortest pump pulses (in our case 43 fs) from the Ti:sapphire laser. However, by adjusting the second-order dispersion of the Ti:sapphire pump laser to increase the pulse duration of the 2.05 μm pump pulses, the conversion efficiency in the second OPA stage of the 5 μm setup was seen to increase. Even though the amplified 2.05 μm pump energy decreases ~0.25 mJ as a result of increasing the pulse duration by 20 fs, the amplified 5 μm pulses increase in energy by ~35 μJ. Accordingly, the pump pulses used in the OPA design have a pulse energy of 1.8 mJ with an rms energy stability of 1.9% measured over three minutes (figure 5(a)) with a uniform beam profile (figure 5(a), inset). Local (spatial/temporal) depletion of the pump in the last OPA stage yields a significant pulse energy stability improvement. The 2.05 μm pump pulse spectrum has been measured to have a FWHM bandwidth of 130 nm, as shown in figure 5(b), potentially supporting a transform-limited autocorrelation FWHM of 42 fs. The autocorrelation of pump pulses has been measured with a FWHM of 63 fs, as shown in figure 5(c). Similar to the 2.05 μm OPA, the spatial overlap in the second OPA stage of the 5 μm setup has been optimized by adjusting the angular orientation of the dichroic beamsplitter immediately before the second OPA to change the noncollinear interaction angle. The optimal noncollinear angle used in the second OPA stage is ~0.9°. By pumping the OPG/OPA system with the pump pulses described, the idler pulses at 5 μm have been produced with a pulse energy of 53 μJ (or 58 μJ before the long-pass filter) and an rms energy stability of 1.6% measured over three minutes, as shown in figure 6(a). The peak-to-peak pulse energy stability was measured to be 15.5%. At the expense of higher output energy from the OPA, the noncollinear angle of the second OPA stage was adjusted to improve the beam quality of the idler pulses (figure 6(a), inset). The amplified pulse spectrum has been measured by a scanning grating spectrometer with an InSb photodiode. As shown in figure 6(b), the spectrum is centered at a wavelength of ~5 μm with a FWHM of 750 nm, potentially supporting a transform-limited pulse duration of ~49 fs, as shown in figure 6(c), with the measured spectrum, assuming a Fourier time-bandwidth product of 0.44.

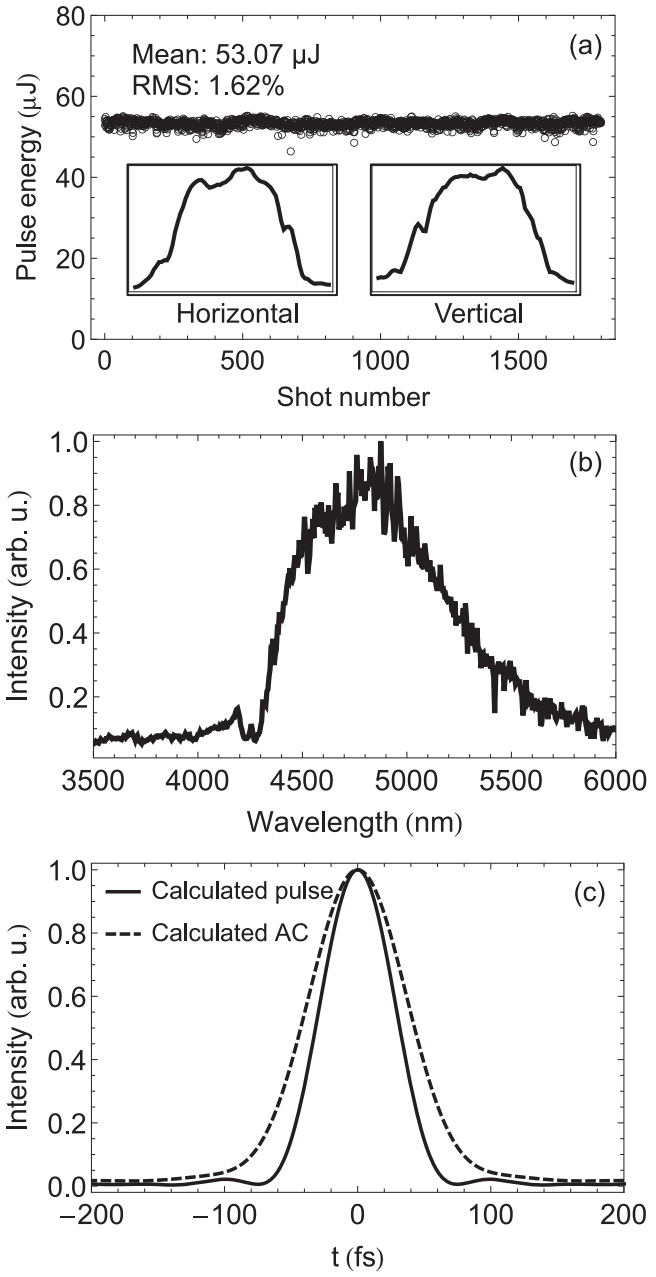

Figure 6. Energy stability of (a) 5 μm idler pulses; inset: horizontal and vertical beam profiles, (b) amplified idler pulse spectrum, and (c) solid line: calculated transform limited pulse shape; dashed line: calculated transform limited autocorrelation.

The near-term experimental priorities for mid-IR source development using our setup include a detailed temporal characterization of amplified 5 μm pulses and increasing the conversion efficiency in the second OPA stage. Due to strong atmospheric absorption near 2.5 μm, measuring the pulse duration in a technique that utilizes SHG, such as autocorrelation, is technically challenging. The absorption issue can be circumvented with little effect on system performance by shifting the output of the mid-IR system to a slightly shorter wavelength (~4.7 μm). At the SHG of this wavelength, the atmospheric absorption is significantly reduced. The system design support this small spectral shift by the change of pump-seed delay and small adjustment of the angles of OPA crystals.

The limited conversion efficiency of the second 5 μm OPA stage is likely caused by several factors. First, a mismatch exists between the pump pulse duration (63 fs) and the preamplified signal pulse that experiences significant dispersion by propagating through a CaF_2 lens and dichroic beamsplitter prior to entering the second OPA. The preamplified signal pulse dispersion is calculated to add a group delay dispersion (GDD) of $-650\,fs^2$. A simple one-dimensional simulation [34] suggests that by managing the seed GDD, the combined signal idler conversion efficiency in the second OPA can be increased. With a small seed GDD, the pulses are short and the effective interaction length is limited by GVM rather than the ZGP crystal length. An increase of seed GDD results in a longer chirped seed pulse compared to the pump pulse. A higher conversion efficiency can be achieved in this case because the pulse splitting length increases. At a certain point, however, the effective interaction length becomes equal to the crystal length, and the gain is reduced since further increase in GDD simply reduces the seed energy available for mixing with the pump pulse. Dispersion tuning of the signal between the two OPA stages can be realized by judicious use of materials such as ZnSe and Ge. The second possible cause for limited conversion efficiency is the nonlinear absorption of the pump in the ZGP crystal, reducing the effective pump intensity. A significant uncertainty of the nonlinear absorption coefficient has been reported in the past work, such that numerical estimates of this effect are not reliable without additional measurement.

6. Conclusion

While much work has been done to date in developing mid-IR sources using OPA and OPCPA, well-characterized ultrashort mid-IR pulses are not commonly avalailable. Major limitations of ultrafast mid-IR technology at the present time include the low level of maturity and availability of nonlinear materials and pump lasers, lack and cost of suitable diagnostics, and sometimes absorption properties both in atmospheric propagation and in optical and nonlinear conversion materials.

The design and preliminary performance of a passively CEP-stabilized 5 μm parametric source utilizing two-stage OPA in ZGP has been presented. The source exhibits high energy (>50 μJ), broad bandwidth (>1000 nm), smooth beam profile, and excellent pulse-to-pulse rms stability of ~1.62%. The development of a 2 μm few-millijoule-level ultrafast surrogate source has also been described, resulting in a well-characterized parametric source based on the use of a compact, commercially available Ti:sapphire laser pump. We expect this scheme to be even more robust, stable, and efficient following the development of direct mid-IR pumping, such as by the use of a Cr:ZnSe laser instead of the surrogate 2 μm pump source driven by a Ti:sapphire laser. In the energy range required for pumping DLA and other applications requiring millijoule-level, sub-ps, mid-IR ultrashort pulses, the demonstrated approach is considerably simpler for implementation than OPCPA. Production of higher-energy ultrashort mid-IR pulses requires the use of a more energy-scalable technique such as OPCPA. At the demonstrated energy level, ultrashort mid-IR laser pulses are nevertheless attractive for other applications as well, such as high-order harmonic generation, attosecond pulse production, and laser–matter interactions.

Acknowledgments

This work was supported by DARPA under Contract No. N66001-11-1-4197.

References

[1] Peralta E A *et al* 2013 *Nature* **503** 91
[2] Tajima T and Dawson J M 1979 *Phys. Rev. Lett.* **43** 267
[3] Rosenzweig J, Murokh A and Pellegrini C 1995 *Phys. Rev. Lett.* **74** 2467
[4] Palastro J P, Antonsen T M, Morshed S, York A G and Milchberg H M 2008 *Phys. Rev.* E **77** 036405
[5] Lin M-W and Jovanovic I 2012 *Phys. Plasmas* **19** 113104
[6] Jauregui C, Limpert J and Tuennermann A 2013 *Nat. Photonics* **7** 861
[7] Naranjo B, Valloni A, Putterman S and Rosenzweig J B 2012 *Phys. Rev. Lett.* **109** 164803
[8] Breuer J and Hommelhoff P 2013 *Phys. Rev. Lett.* **111** 134803
[9] Moulton P and Slobodchikov E 2011 *CLEO:2011—Laser Applications to Photonic Applications* OSA Technical Digest (CD) (Baltimore, MD) paper PDPA10
[10] Tolstik N, Sorokin E and Sorokina I 2013 *Opt. Lett.* **38** 299
[11] Stutzki F, Jansen F, Jauregui C, Limpert J and Tuennermann A 2013 *Opt. Lett.* **38** 97
[12] Bradler M, Homann C and Riedle E 2011 *Opt. Lett.* **36** 4212
[13] di Trapani P, Andreoni A, Banfi G P, Solcia C, Danielius R, Piskarskas A, Foggi P, Monguzzi M and Sozzi C 1995 *Phys. Rev.* A **51** 3164
[14] Danielius R, Piskarskas A, di Trapani P, Andreoni A, Solcia C and Foggi P 1996 *Opt. Lett.* **21** 973
[15] Dubietis A, Jonusauskas G and Piskarskas A 1992 *Opt. Commun.* **88** 437
[16] Jovanovic I, Comaskey B J, Ebbers C A, Bonner R A, Pennington D M and Morse E C 2002 *Appl. Opt.* **41** 2923
[17] Ishii N, Teisset C Y, Fuji T, Kohler S, Schmid K, Veisz L, Baltuska A and Krausz F 2006 *IEEE J. Sel. Top. Quantum Electron.* **12** 173

[18] Andriukaitis G, Balciunas T, Alisauskas S, Pugzlys A, Baltuska A, Popmintchev T, Chen M-C, Murnane M and Kapteyn H 2011 *Opt. Lett.* **36** 2755
[19] Deng Y *et al* 2012 *Opt. Lett.* **37** 4973
[20] Petrov V, Rotermund F, Noack F and Schunemann P 1999 *Opt. Lett.* **24** 414
[21] Biegert J, Chalus O and Bates P 2010 *Coherence and Ultrashort Pulse Laser Emission* (Rijeka: InTech)
[22] Elezzabi A Y, Meyer J, Hughes M K Y and Johnson S R 1994 *Opt. Lett.* **19** 898
[23] Silva F, Bates P K, Esteban-Martin A, Ebrahim-Zadeh M and Biegert J 2012 *Opt. Lett.* **37** 933
[24] Schmidt B E, Shiner A D, Lassonde P, Kieffer J-C, Corkum P B, Villeneuve D M and Legare F 2011 *Opt. Express* **19** 6858
[25] Adhav R S, Adhav S R and Pelaprat J M 1987 *Laser Focus* **23** 88
[26] Castech 2012 *Crystals catalog* 21 'NLO Crystals'
[27] Hansson G, Karlsson H, Wang S and Laurell F 2000 *Appl. Opt.* **39** 5058
[28] Peterson R D, Schepler K L, Brown J L and Schunemann P G 1995 *J. Opt. Soc. Am.* B **12** 2142
[29] Rotermund F, Petrov V and Noack F 2000 *Opt. Commun.* **185** 177
[30] Skauli T *et al* 2002 *Opt. Lett.* **27** 628
[31] Xu G, Wandel S and Jovanovic I 2014 *Rev. Sci. Instrum.* **85** 023102
[32] Cerullo G and de Silvestri S 2003 *Rev. Sci. Instrum.* **74** 1
[33] Schunemann P G, Budni P A, Pomeranz L, Knights M G, Pollak T M and Chicklis E P 1997 *Advanced Solid-State Lasers (Trends in Optics and Photonics Series* vol 10) ed C R Pollock and W R Bosenberg (Washington, DC: Optical Society of America) p 253
[34] Yin Y C, French D and Jovanovic I 2010 *Opt. Express* **18** 18471